62nd Annual Technical Conference Proceedings
Long Beach, California, USA, April 29 - May 2, 2019
https://doi.org/10.14332/svc19.proc.0046

 ISSN 0737-5921
ISBN 978-1-878068-39-2

Oxidation of Aluminum Protected by Wide Band Gap MgF_2 Layers as Followed by X-ray Photoelectron Spectroscopy

Brian I. Johnson[a], Tahereh Gholian Avval[a], Grant P. Hodges[a], Karen Membreno[a], David D. Allred[b], Matthew R. Linford[a]
[a] Department of Chemistry and Biochemistry, Brigham Young University, C100 BNSN, Provo,Utah 84602
[b] Department of Physics and Astronomy, Brigham Young University, N265 ESC, Provo,Utah 84602

ABSTRACT

Aluminum enjoys broad band reflectivity and is widely used as an astronomical reflector. However, it oxides rapidly, and this oxide absorbs very short wavelength light, which limits the performance of aluminum mirrors. Accordingly, thin transparent layers, such as films of MgF_2, are used to protect aluminum. In this study, we present an X-ray photoelectron spectroscopy (XPS) study of the chemical changes in MgF_2 - protected aluminum that take place as it oxidizes (is exposed to the air). XPS reveals the rate of Al oxidation for different MgF_2 thicknesses as determined from measurements obtained from 5 min to 8 months of air exposure. The degree of Al oxidation depends on the MgF_2 over layer thickness.

INTRODUCTION

Aluminum has unique properties and numerous applications [1-3]. It is generally considered to be an easy metal to work with. It has a relatively low melting point, it is ductile yet strong enough to be used in structural applications, it is lightweight, it can be alloyed, and it is unmatched in its ability to reflect light over a wide energy range [4]. A drawback to aluminum is that its surface oxidizes quickly. Of course, a small amount of oxide is not a limitation for most of aluminum's applications. However, aluminum oxide, even when only a few nanometers thick, absorbs short wavelength light, which significantly limits aluminum's ability to act as a space mirror and collect light over the widest possible wavelength range [5-9]. Because of the importance of aluminum and aluminum oxide, these materials have previously been studied by various experimental and theoretical methods, including X-ray photoelectron spectroscopy (XPS) [10-15].

A general strategy for preventing aluminum from oxidizing while preserving its optical properties is to coat it with a wide band gap material [16-19]. These types of barrier layers, e.g., MgF_2 and other inorganic salts, have been used for decades to protect aluminum reflectors, including those in the Hubble space telescope [5, 20-24]. Indeed, aluminum is currently being proposed as the primary reflector for future space missions such as the LUVOIR project, which will be the flagship NASA space observatory for the 2020s and 2030s. However, in spite of the importance of protecting aluminum mirrors, we are not aware of any systematic XPS analysis of MgF_2-protected aluminum mirrors. Here we present such a study. We show that XPS can be used to follow aluminum oxidation under MgF_2 layers of varying thickness, and that its oxidation rate depends on the thickness of the MgF_2 over it, i.e., thicker MgF_2 films result in slower Al oxidation. This document follows our recent, related conference proceedings on the spectroscopic ellipsometry (SE) analysis of the oxidation of MgF_2-protected aluminum [25].

EXPERIMENTAL

2.1. Instrumentation

XPS was performed with a Surface Science SSX-100 instrument (maintained by Service Physics, Bend, OR, USA) with a hemispherical analyzer. The instrument employs monochromatic Al Kα X-rays. Survey scans were collected with an X-ray spot size of 800 x 800 μm^2, an instrument resolution of '4', a nominal pass energy of 150 eV, 6 passes/scan, and a step size of 1 eV [23, 24]. High resolution (narrow) scans were collected over the Al 2s region, centered at a binding energy of 120 eV, with an energy window of 40 eV, and a step size of 0.0625 eV. The number of scans ranged between 15 and 35, and the spot size was 800 x 800 μm^2 with an instrument resolution of '3' (nominal pass energy of 100 eV). Area ratios were calculated using the CasaXPS modelling/fitting software (Casa Software Ltd., Version 2.3.18PR1.0). SE (M-2000D, J.A. Woollam, Lincoln, NE, USA, wavelength range: ca. 190-1688 nm, CompleteEASE data analysis software) was used to measure the thicknesses of model/calibration MgF_2 layers on previously characterized silicon substrates. Data were acquired at 75°. Modeling was performed with the optical functions in the instrument software for MgF_2 (MgF_2E (Sellmeier)) and Si/SiO_2 (Si_JAW and SIO2_JAW, respectively).

62nd Annual Technical Conference Proceedings
Long Beach, California, USA, April 29 - May 2, 2019
https://doi.org/10.14332/svc19.proc.0046

ISBN 978-1-878068-39-2

2.2. Deposition of Al and MgF_2

Four sets of aluminum films were deposited using a Denton (Morristown, NJ) DV-502 A thermal evaporator. This evaporator uses two independent resistance-heated sources for depositions and a rotating stage to ensure even depositions. An Inficon (Bad Ragaz, Switzerland) quartz-crystal monitor (QCM) in the chamber made in situ thickness measurements so that the system could automatically close a shutter assembly to end depositions. The thickness values from the QCM (previously calibrated) were used in this study for the MgF_2 thicknesses. For each sample preparation, a 1" piece of aluminum wire was placed into a tungsten resistance heater coil and a molybdenum boat was filled with ca. 15 g of MgF_2. Prior to deposition, the system was pumped to a base pressure of 4 x 10^{-6} torr and the Al was deposited at a rate of 35 Å/sec to achieve a thickness of 150 Å. The MgF_2 was then immediately deposited onto the Al at a rate of 3 Å/sec. The time for both depositions was 35–45 s. Immediately following the depositions of Al and MgF_2, the chamber was vented with N_2(g), which took 1.5 – 2 min. The samples were then removed and rushed to the SE and XPS instruments for analysis. Samples were timed from chamber removal to the beginning of SE or XPS analysis. Each sample was divided into multiple pieces: one piece for SE analysis and the others for XPS.

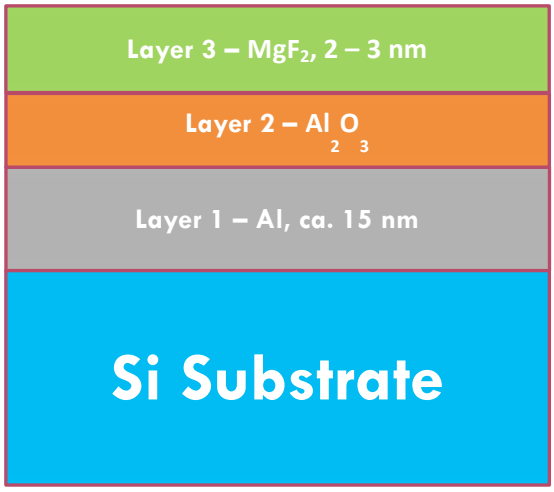

Figure 1. Model of the stack deposited and analyzed in this study (not to scale).

RESULTS AND DISCUSSION

3.1. XPS Analysis

XPS is a surface sensitive technique that probes the upper 5 – 10 nm of materials. It yields elemental compositions and oxidation states[20]. XPS Al 2s narrow scans of MgF_2 – protected Al (see Fig. 1) were modeled by peak fitting, which is often essential in XPS data analysis because the natural line widths in XPS are often comparable to the chemical shifts for the elements [26].

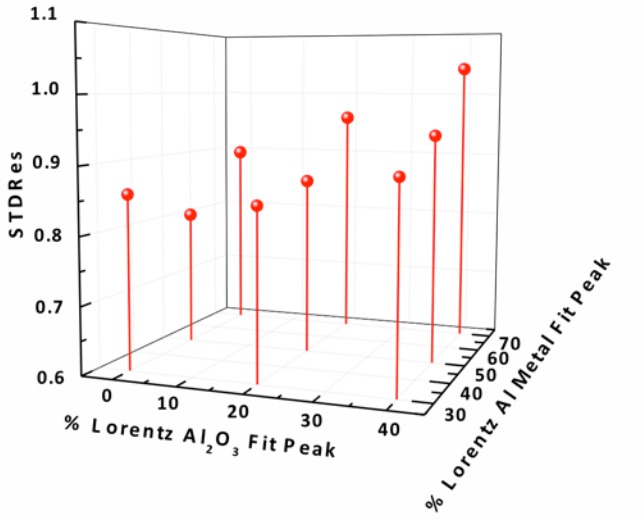

Figure 2. The standard deviation of the residuals (STDRes) for fits of the Al 2s XPS narrow scans as a function of the Lorentzian character in the Al_2O_3 (oxide) and Al (metal) fit components. These values are the averages of fits to 27 narrow scans.

To study the oxidation rate of Al as a function of MgF_2 thickness, we examined the Al 2s signal at ca. 118 eV. The Al 2s and 2p peaks are the most intense signals from Al. We chose the Al 2s region for simplicity, i.e., so that we would not need to consider spin-orbit splitting, which should be accounted for in Al 2p peak analysis. For the peak fitting, two types of pseudo Voigt synthetic line shapes were considered: Gaussian-Lorentzian product (GLP) and Gaussian-Lorentzian sum (GLS) functions [22]. Ultimately, we used GLS line shapes because they fitted our data better than the GLP functions. As expected, the lower energy component in the Al 2s narrow scans attributable to the unoxidized (metallic) Al film exhibited greater Lorentzian character and was narrower than the peak that accounted for the oxide in the material – we attribute the greater width (FWHM) of the oxide signal to disorder in the oxide and phonon broadening [27]. To obtain the best fits to the narrow scans, we varied the Lorentzian character of both fit components to minimize the standard deviation of the residuals (STDRes) to the fit. This analysis (see Fig. 2) yielded best values of the Lorentzian character/fraction in the GLS line shapes of 50% and 0% for the Al and Al_2O_3 fit components, respectively. These values were used in the remainder of this study.

62nd Annual Technical Conference Proceedings
Long Beach, California, USA, April 29 - May 2, 2019
https://doi.org/10.14332/svc19.proc.0046

 ISSN 0737-5921
ISBN 978-1-878068-39-2

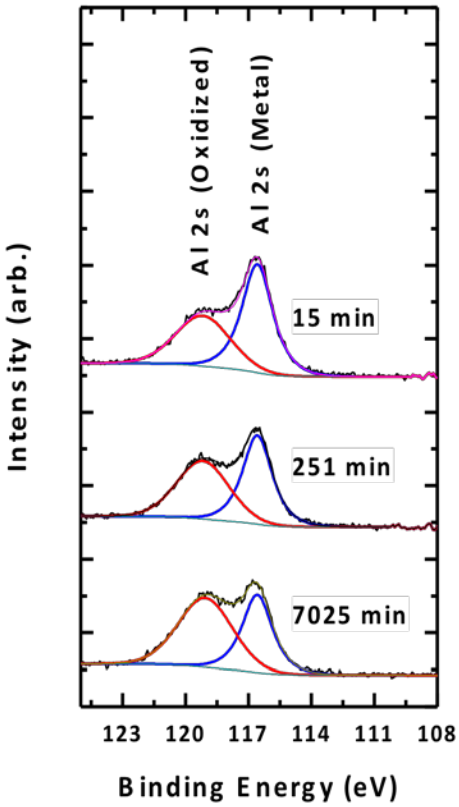

Figure 3. Representative Al 2s narrow scans from MgF_2 – coated Al as a function of air exposure time.

XPS spectra of MgF_2-covered Al layers were acquired as a function of time. For example, Fig. 3 shows representative Al 2s narrow scans taken at three air exposure times. Oxidation of the Al layer is clearly taking place here, as evidenced by the steady increase in the Al_2O_3 to Al area ratio. In spite of the fact that neither the separation nor the full width at half maximum (FWHM) values for the Al and Al_2O_3 fit components were constrained in any of these fits, the average FWHM values for the Al and Al_2O_3 fit components across the fits were very similar: 1.72 ± 0.07 eV and 2.98 ± 0.13 eV, respectively, which is consistent with these peak envelopes being well described by the two proposed components. These FWHM values are within 10% of respective literature values for γ-Al_2O_3, and within 15% for Al metal[26-29]. In addition, the energy difference between the Al_2O_3 and Al fit components was quite constant: 2.57 ± 0.12 eV, as was the ratio between them (see Table 1). These results suggest that our model for analyzing the Al 2s peak envelope was reasonable.

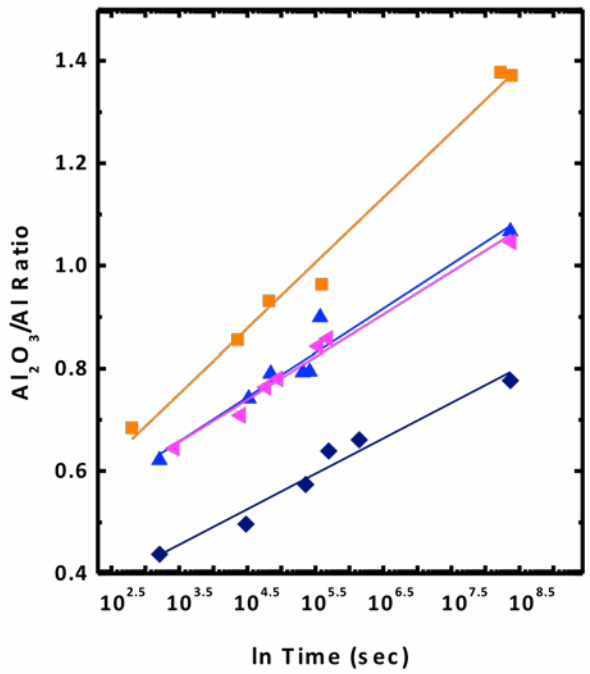

Figure 4. XPS Al_2O_3/Al ratios as a function of air exposure time as fit to the following lines:
- 1.82 nm MgF_2: y=0.0637 ln(x)+0.305
- 2.20 nm MgF_2:y=0.0414 ln(x)+0.367
- 2.30 nm MgF_2: y=0.0431 ln(x)+0.356
- 3.08 nm MgF_2: y=0.0346 ln(x)+0.214

Figure 4 shows the Al_2O_3/Al fit component ratios from MgF_2 -protected samples exposed to the air for between 5 min and 8

Table 1. Average FWHM values, peak energy (BE) differences, and ratios of FWHM values for the Al and Al_2O_3 fit components in the Al 2s narrow scans considered in this study.

MgF_2 Thickness (nm)	Average FWHM Al 2s Peak	Average FWHM Al_2O_3 2s Peak	Average BE Difference Al-Al_2O_3 2s Peaks	Average FWHM Ratio Al_2O_3 /Al 2s Peaks
1.82	1.76 ± 0.14	2.96 ± 0.14	2.49 ± 0.1	1.68 ± 0.09
2.20	1.68 ± 0.06	2.82 ± 0.08	2.59 ± 0.08	1.68 ± 0.08
2.30	1.74 ± 0.04	2.99 ± 0.08	2.46 ± 0.04	1.72 ± 0.06
3.08	1.71 ± 0.04	3.15 ± 0.22	2.75 ± 0.24	1.84 ± 0.16
Average	**1.72 ± 0.07**	**2.98 ± 0.13**	**2.57 ± 0.12**	**1.73 ± 0.09**

62nd Annual Technical Conference Proceedings
Long Beach, California, USA, April 29 - May 2, 2019
https://doi.org/10.14332/svc19.proc.0046

ISBN 978-1-878068-39-2

months. Reasonable linear fits to the data are obtained by relating the Al_2O_3/Al area ratio to the logarithm of time, as follows:

(1) $Al_2O_3/Al = m \ln t + b$

where m and b are the slope and intercept of this line. It is significant that (i) both the Al_2O_3/Al ratios and m values (slopes) are smallest for the thickest over layers of MgF_2, which confirms their ability to slow aluminum oxidation, and (ii) oxidation appears to continue over the entire exposure of the samples to the air. To further emphasize the decrease in oxidation with increasing over layer thickness, the m values (slopes) for the lines in Fig. 4 are plotted in Fig. 5 as functions of MgF_2 thickness.

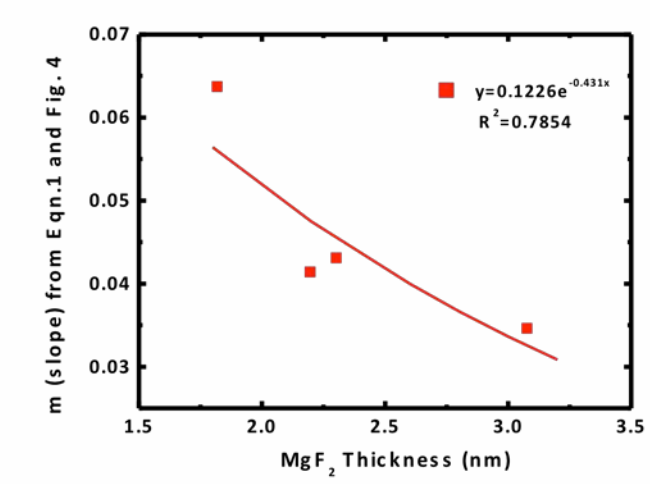

Figure 5. Values of m determined from Equation 1 and Fig. 4. In large measure, the fit to these values here should be considered a guide to the eye.

CONCLUSIONS

The effects of MgF_2 thickness on the oxidation rate of aluminum was determined by XPS. The raw data showed that as the MgF_2 thickness increased, the oxidation rate of aluminum decreased. Good fits to the Al 2s narrow scans were obtained with relatively few constraints. The Gaussian-Lorentzian sum functions used to model the Al_2O_3 and Al peaks in the Al 2s narrow scans had 0% and 50% Lorentzian character, respectively. Plots of the Al_2O_3/Al ratios as a function air exposure time showed that oxidation increased in a logarithmic fashion that depended on the thickness of the MgF_2 over layer.

ACKNOWLEDGEMENTS

The authors gratefully thank and acknowledge the Utah NASA Space Grant Consortium for funding this work, and also SVC for a travel award to BIJ to attend the SVC conference in Long Beach, CA in 2019.

REFERENCES

[1] M. Bertram, K. J. Martchek, and G. Rombach, "Material flow analysis in the aluminum industry," *Journal of Industrial Ecology,* vol. 13, no. 5, pp. 650-654, 2009. doi.org/10.1111/j.1530-9290.2009.00158.x

[2] S. Das and W. Yin, "Trends in the global aluminum fabrication industry," *JOM,* vol. 59, no. 2, pp. 83-87, 2007. doi.org/10.1007/s11837-007-0027-2

[3] M. Skillingberg and J. Green, "Aluminum applications in the rail industry," *LIGHT METAL AGE-CHICAGO-,* vol. 65, no. 5, p. 8, 2007. http://citeseerx.ist.psu.edu/viewdoc/download?doi=10.1.1.728.9874&rep=rep1&type=pdf

[4] G. Hass and R. Tousey, "Reflecting coatings for the extreme ultraviolet," *JOSA,* vol. 49, no. 6, pp. 593-602, 1959doi.org/10.1364/JOSA.49.000593.

[5] F. Bridou, M. Cuniot-Ponsard, J.-M. Desvignes, I. Maksimovic, and P. Lemaire, "VUV mirrors for the (80-120 nm) spectral range," in *Advances in Optical Thin Films*, 2004, vol. 5250: International Society for Optics and Photonics, pp. 627-637. doi.org/10.1117/12.514441

[6] H. Brune, J. Wintterlin, R. Behm, and G. Ertl, "Surface migration of ‘‘hot’’adatoms in the course of dissociative chemisorption of oxygen on Al (111)," *Physical review letters,* vol. 68, no. 5, p. 624, 1992. doi.org/10.1103/PhysRevLett.68.624

[7] T. Do, N. McIntyre, R. Harshman, M. Lundy, and S. Splinter, "Application of parallel factor analysis and x‐ray photoelectron spectroscopy to the initial stages in oxidation of aluminium. I. The Al 2p photoelectron line," *Surface and interface analysis,* vol. 27, no. 7, pp. 618-628, 1999. doi.org/10.1002/(SICI)1096-9918(199907)27:7<618::AID-SIA550>3.0.CO;2-7

[8] J. Trost, H. Brune, J. Wintterlin, R. Behm, and G. Ertl, "Interaction of oxygen with Al (111) at elevated temperatures," *The Journal of chemical physics,* vol. 108, no. 4, pp. 1740-1747, 1998. doi.org/10.1063/1.475546

[9] Y. F. Zhukovskii, P. Jacobs, and M. Causá, "On the mechanism of the interaction between oxygen and close-packed single-crystal aluminum surfaces," *Journal of Physics and Chemistry of Solids,* vol. 64, no. 8, pp. 1317-1331, 2003. doi.org/10.1016/S0022-3697(03)00156-2

[10] T. Do, S. Splinter, C. Chen, and N. McIntyre, "The oxidation kinetics of Mg and Al surfaces studied by AES

https://doi.org/10.14332/svc19.proc.0046
 ISSN 0737-5921
ISBN 978-1-878068-39-2

and XPS," *Surface Science,* vol. 387, no. 1-3, pp. 192-198, 1997. doi.org/10.1016/S0039-6028(97)00351-8

[11] M. Fernández-Perea, J. I. Larruquert, J. A. Aznárez, A. Pons, and J. A. Méndez, "Vacuum ultraviolet coatings of Al protected with MgF 2 prepared both by ion-beam sputtering and by evaporation," *Applied optics,* vol. 46, no. 22, pp. 4871-4878, 2007. doi.org/10.1364/AO.46.004871

[12] I. Lazić and B. J. Thijsse, "An improved molecular dynamics potential for the Al–O system," *Computational Materials Science,* vol. 53, no. 1, pp. 483-492, 2012. doi.org/10.1016/j.commatsci.2011.08.021

[13] N. Madaan *et al.*, "Al2O3 e-Beam Evaporated onto Silicon (100)/SiO2, by XPS," *Surface Science Spectra,* vol. 20, no. 1, pp. 43-48, 2013. doi.org/10.1116/11.20121102

[14] S. S. Kanyal, D. S. Jensen, Z. Zhu, and M. R. Linford, "Al2O3 e-beam evaporated onto silicon (100)/SiO2 by ToF-SIMS," *Surface Science Spectra,* vol. 22, no. 2, pp. 7-13, 2015. doi.org/10.1116/1.4930928

[15] P. M. Sherwood, "Curve fitting in surface analysis and the effect of background inclusion in the fitting process," *Journal of Vacuum Science & Technology A: Vacuum, Surfaces, and Films,* vol. 14, no. 3, pp. 1424-1432, 1996. doi.org/10.1116/1.579964

[16] L. V. R. De Marcos *et al.*, "Optimization of MgF 2-deposition temperature for far UV Al mirrors," *Optics express,* vol. 26, no. 7, pp. 9363-9372, 2018. doi.org/10.1364/OE.26.009363

[17] B. Fateh, G. A. Brooks, M. Rhamdhani, J. Taylor, J. Davis, and M. Lowe, "Study of Early Stage Interaction of Oxygen with Al; Methods, Challenges and Difficulties," in *Light Metals 2011*: Springer, 2011, pp. 725-730. doi.org/10.1007/978-3-319-48160-9_126

[18] C. M. Lousada and P. A. Korzhavyi, "First stages of oxide growth on Al (1 1 0) and core-level shifts from density functional theory calculations," *Applied Surface Science,* vol. 441, pp. 174-186, 2018. doi.org/10.1016/j.apsusc.2018.01.246

[19] S. Wilbrandt, O. Stenzel, H. Nakamura, D. Wulff-Molder, A. Duparré, and N. Kaiser, "Protected and enhanced aluminum mirrors for the VUV," *Applied optics,* vol. 53, no. 4, pp. A125-A130, 2014. doi.org/10.1364/AO.53.00A125

[20] V. Gupta, H. Ganegoda, M. H. Engelhard, J. Terry, and M. R. Linford, "Assigning oxidation states to organic compounds via predictions from X-ray photoelectron spectroscopy: a discussion of approaches and recommended improvements," *Journal of Chemical Education,* vol. 91, no. 2, pp. 232-238, 2013. doi.org/10.1021/ed400401c

[21] G. Hass, "Filmed surfaces for reflecting optics," *JOSA,* vol. 45, no. 11, pp. 945-952, 1955. doi.org/10.1364/JOSA.45.000945

[22] V. Jain, M. C. Biesinger, and M. R. Linford, "The Gaussian-Lorentzian Sum, Product, and Convolution (Voigt) functions in the context of peak fitting X-ray photoelectron spectroscopy (XPS) narrow scans," *Applied Surface Science,* vol. 447, pp. 548-553, 2018. doi.org/10.1016/j.apsusc.2018.03.190

[23] D. Shah *et al.*, "Tutorial on interpreting x-ray photoelectron spectroscopy survey spectra: Questions and answers on spectra from the atomic layer deposition of Al2O3 on silicon," *Journal of Vacuum Science & Technology B, Nanotechnology and Microelectronics: Materials, Processing, Measurement, and Phenomena,* vol. 36, no. 6, p. 062902, 2018. doi.org/10.1116/1.5043297

[24] S. Tougaard, "Improved XPS analysis by visual inspection of the survey spectrum," *Surface and Interface Analysis,* vol. 50, no. 6, pp. 657-666, 2018. doi.org/10.1002/sia.6456

[25] B. I. Johnson, T. Gholian Avval, G. Hodges, K. Membreno, D. D. Allred, and M. R. Linford, "Real-Time Monitoring of Aluminum Oxidation Through Wide Band Gap MgF2 Layers for Protection of Space Mirrors," in *2019 25th Annual Fellowship Symposium*, Brigham Young University, 2019: Utah NASA Space Grant Consortium.

[26] D. M. Wyatt, R. C. Gray, J. C. Carver, D. M. Hercules, and L. W. Masters, "Studies of Polymeric Bond Failure on Aluminum Surfaces by X-ray Photoelectron Spectroscopy (ESCA)," *Applied Spectroscopy,* vol. 28, no. 5, pp. 439-445, 1974. doi.org/10.1366/000370274774332146

[27] J. A. Rotole and P. M. Sherwood, "Gamma-alumina (γ-Al2O3) by XPS," *Surface Science Spectra,* vol. 5, no. 1, pp. 18-24, 1998. doi.org/10.1116/1.1247852

[28] B. R. Strohmeier, "Gamma‐Alumina (γ‐Al2O3) by XPS," *Surface Science Spectra,* vol. 3, no. 2, pp. 135-140, 1994. doi.org/10.1116/1.1247774

[29] J. A. Rotole and P. M. Sherwood, "Corrundum (α-Al2O3) by XPS," *Surface Science Spectra,* vol. 5, no. 1, pp. 11-17, 1998. doi.org/10.1116/1.1247851

FOR FURTHER INFORMATION

Contact the author, Brian Johnson, at bjohns42@byu.edu